Katholieke Universiteit Leuven

Departement Elektrotechniek

ESAT-SISTA/TR 04-74

Data Assimilation in 2D Magneto-Hydrodynamics Systems [1]

Oscar Barrero Mendoza, Dennis S. Bernstein[2], and Bart L.R. De Moor[3].

September 17, 2004

[1] This report is available by anonymous ftp from *ftp.esat.kuleuven.ac.be* in the directory *pub/sista/barrero/reports/report04-156.ps.gz*

[2] Dr. Dennis S. Berstein is a full professor at the Department of Aerospace Engineering, The University of Michigan, Ann Arbor, MI 48109-2140, USA

[3] Dr. Bart De Moor is a full professor at the Katholieke Universiteit Leuven, Belgium. Research supported by Research Council KUL: GOA-Mefisto 666, GOA-Ambiorics, several PhD/postdoc & fellow grants; Flemish Government: - FWO: PhD/postdoc grants, projects, G.0240.99 (multilinear algebra), G.0407.02 (support vector machines), G.0197.02 (power islands), G.0141.03 (Identification and cryptography), G.0491.03 (control for intensive care glycemia), G.0120.03 (QIT), G.0452.04 (QC), G.0499.04 (robust SVM), research communities (ICCoS, ANMMM, MLDM); - AWI: Bil. Int. Collaboration Hungary/ Poland; - IWT: PhD Grants, GBOU (McKnow) Belgian Federal Government: Belgian Federal Science Policy Office: IUAP V-22 (Dynamical Systems and Control: Computation, Identification and Modelling, 2002-2006), PODO-II (CP/01/40: TMS and Sustainibility); EU: FP5-Quprodis; ERNSI; Eureka 2063-IMPACT; Eureka 2419-FliTE; Contract Research/agreements: ISMC/IPCOS, Data4s, TML, Elia, LMS, IPCOS, Mastercard;

Abstract

Prediction of solar storms has become a very important issue due to the fact that they can affect dramatically the telecommunication and electrical power systems in the earth. As a result, a lot of research is being doing in this direction, *space weather forecast*. Magneto-Hydrodynamics systems are being studied in order to analyze the space plasma dynamics, and techniques which have been broadly used in prediction of earth environmental variables like the Kalman filter (KF), the ensemble Kalman filter (EnKF), the extended Kalman filter (EKF), etc., are being studied and adapted to this new framework. The assimilation of a wide range of space environment data into first-principles based global numerical models will improve our understanding of the physics of the geospace environment and the forecasting of its behaviour. Therefore, the aim of this paper is to study the performance of nonlinear observers in Magneto-Hidrodynamics systems, namely, the EnKF.

The EnKF is based on a Monte Carlo simulation approach for propagation of process and measurement errors. In this paper, the EnKF for a nonlinear two-dimensional magneto-hydrodynamic (2D-MHD) system is considered. For its implementation, two software packages are merged, namely, the Versatile Advection Code (VAC) written in Fortran and Matlab of Mathworks. The 2D-MHD is simulated with the VAC code while the EnKF is computed in Matlab. In order to study the performance of the EnKF in MHD systems, different number of measurement points as well as ensemble members are set.

1 Introduction

In this paper, a first attempt is done for investigating the performance of the EnKF [4] in space weather forecast. Space weather forecast is an area of research that has become very active in the last years due to the need to predict solar storms. This solar storms can affect dramatically the telecommunication and electrical power systems in the earth. To predict such events data assimilation techniques can be used, data assimilation consists of combining physical first principle based models with measurements of the physical variables in order to correct the estimation of these ones made by the model, due to the lack of information about initial conditions, boundary conditions, wrong and non-modelled dynamics, etc. Hence, in order to make data assimilation for space weather, MHD equations are used as basis for the physical first principle based model while EnKF for correcting the estimation of the physical variables.

One of the motivation for using the EnKF is that it is very easy to implement due to the fact that it is not needed any model linearization like the extended Kalman filter (EKF). Therefore, the EnKF can be set mainly into two modules; the model simulator and the data assimilation module. These facts make the EnKF very attractive for real applications. Hence, in this paper we use the VAC code [8] as the MHD simulator module and Matlab for the data assimilation module. Finally, the two codes are run simultaneously using a script written in Matlab.

This paper is organized as follows, in the 2^{nd}, 3^{rd} and 4^{th} sections the MHD system and EnKF are introduced respectively. In the 5^{th} section numerical results are presented and finally in the 6^{th} section some conclusions are given.

2 MHD system equations

The topic of MHD is ubiquitous in plasma physics. Examples where the theory has been used with success range from explaining the spontaneous generation and subsequent evolution of magnetic fields within stellar and planetary interiors, to accounting for the gross stability of magnetically confined thermonuclear plasmas. Often, it is found that the scale length of many instabilities and waves which are able to grow or propagate in a system are comparable with the plasma size. It transpires that MHD is capable of providing a good description of such large scale disturbances, indicating that the MHD account of plasma behaviour is necessarily a macroscopic one. In essence, the theory is a marriage between fluid mechanics and electromagnetism. When compared with the extremely detailed particle and kinetic theories, MHD is a relatively simple theory, perhaps even crude. Despite its apparent simplicity, MHD describes a remarkably rich and varied mix of phenomena and the subject is one whose development continues to flourish [2].

The basic equations of MHD can be summarized as follows:

mass continuity:

$$\frac{\partial \rho}{\partial t} + \nabla \cdot (\rho, \upsilon) = 0, \tag{1}$$

adiabatic equation of state:

$$\frac{d}{dt}\left(\frac{p}{\rho^{\gamma}}\right) = 0, \tag{2}$$

momentum equation,

$$\rho \frac{d\upsilon}{dt} = J \times B - \nabla p, \tag{3}$$

Ampere's law:

$$\nabla \times B = \mu_0 J, \tag{4}$$

Faraday's law:

$$\nabla \times E = -\frac{\partial B}{\partial t}, \tag{5}$$

Gauss' law:

$$\nabla \cdot B = 0, \tag{6}$$

resistive Ohm's law:

$$E + \upsilon \times B = \eta J, \tag{7}$$

where each of the symbols has its customary meaning (see the list of symbols below), with the convective derivative

$$\frac{d}{dt} \triangleq \frac{\partial}{\partial t} + \upsilon \cdot \nabla$$

On the other hand, the right-hand side of (7) may be neglected to yield the ideal Ohm's law:

$$E + \upsilon \times B = 0 \tag{8}$$

This states that there is no electric field in the rest frame of the fluid. Equations (1)-(6) with (8) constitute the ideal MHD equations, which is usually contracted to MHD. The inclusion of (7) is described as resistive MHD.

An enormous amount of physics has been discarded in obtaining the MHD equations, so it is pertinent to enquire what precisely has been retained. It can be seen that the equations are essentially an amalgam of fluids mechanics and 'pre-Maxwell' electromagnetism. The fluid inertia is affected by forces due to the fluid pressure gradients and to the $J \times B$ term, which is the Lorentz force in continuum form. It will be noted however that the Ohm's law couples the fluid to the fields. If the magnetic flux is conserved, then this equation provides constraints on the allowable class of fluid displacements described by the theory, and this in turn has implications for the topology of the magnetic fields.

MHD possesses those conservation properties enjoyed by fluid mechanics and electromagnetism, namely:

- conservation of mass,
- conservation of momentum,

- conservation of energy (both mechanical and electromagnetic),
- conservation of magnetic flux.

list of symbols

μ_0 - permeability of free space (N A^2)
η - resistivity of plasma
ρ - average mass density of plasma (kg/m^3)
p - pressure (N/m^2)
γ - ratio of specific heats
v - velocity of the fluid element (m/s)
J - current density (A/m^2)
E - electric field
B - magnetic field

3 The Kalman Filter

Given a linear dynamical model on discrete form as

$$x_{k+1} = A_k x_k + B_k u_k + w_k, \quad k \geq 0, \tag{9}$$

with output

$$y_k = C_k x_k + v_k, \tag{10}$$

where $x_k \in \mathbb{R}^n$, $u_k \in \mathbb{R}^m$, $y_k \in \mathbb{R}^p$, and A_k, B_k, C_k are known real matrices of appropriate size. The input u_k and output y_k are assumed to be measured, and $w_k \in \mathbb{R}^{n_k}$ and $v_k \in \mathbb{R}^p$ are uncorrelated white noise processes with known variances and correlation given by $Q_k, and R_k$, respectively.

3.1 Estimation Problem

Consider the discrete-time dynamical system described by (9) and (10). For this system, we take a state estimator of the form

$$\hat{x}_{k|k} = \hat{x}_{k|k-1} + L_k(y_k - \hat{y}_{k|k-1}), \quad k \geq 0, \tag{11}$$

where $L_k \in \mathbb{R}^{n \times m}$ and $\hat{x}_{k|k-1}$ is the estimate of x_k based on observations up to time $k-1$, with output

$$\hat{y}_{k|k-1} = C\hat{x}_{k|k-1}. \tag{12}$$

In order to solve this problem a recursive procedure is used. The first step, is to project ahead $x_{k-1|k-1}$ using (9)

$$\hat{x}_{k|k-1} = A_{k-1} x_{k-1|k-1} + B_{k-1} u_{k-1}, \tag{13}$$

then, define the prior state estimation error by

$$e_{k|k-1} \stackrel{\triangle}{=} x_k - \hat{x}_{k|k-1},\ k > 0. \tag{14}$$

Substituting (13) and (9) into (14) we obtain

$$e_{k|k-1} = A_{k-1}e_{k-1|k-1} + w_{k-1}, \tag{15}$$

now, define the prior error covariance matrix by

$$P_{k|k-1} \stackrel{\triangle}{=} E[e_{k|k-1}e_{k|k-1}^{\mathrm{T}}], \tag{16}$$

hence,

$$P_{k|k-1} = A_{k-1}P_{k-1|k-1}A_{k-1}^{\mathrm{T}} + Q_{k-1}. \tag{17}$$

Next, define the state estimator error

$$e_{k|k} \stackrel{\triangle}{=} x_k - \hat{x}_{k|k}, \tag{18}$$

consequently, the Kalman gain L_k minimizes

$$J_k(L_k) = tr(P_{k|k}), \tag{19}$$

where the estimation error covariance matrix $P_{k|k} \in \mathbb{R}^{n\times n}$

$$P_{k|k} \stackrel{\triangle}{=} E[(e_{k|k} - E[e_{k|k}])(e_{k|k} - E[e_{k|k}])^T]. \tag{20}$$

As a result, the Kalman gain can be obtained by

$$L_k = P_{k|k-1}C_k^T(R_k + C_kP_{k|k-1}C_k^T)^{-1}, \tag{21}$$

with the error covariance matrix update

$$P_{k|k} = (I_n - L_kC_k)P_{k|k-1}. \tag{22}$$

Summarizing the algorithm we have for $k = 1, 2, \ldots$

1. Project ahead the error covariance matrix and the estimated states:

$$P_{k|k-1} = A_{k-1}P_{k-1|k-1}A_{k-1}^{\mathrm{T}} + Q_{k-1}$$
$$\hat{x}_{k|k-1} = A_{k-1}\hat{x}_{k-1|k-1} + B_{k-1}u_{k-1}$$

2. Compute the Kalman gain:

$$L_k = P_{k|k-1}C_k^T(R_k + C_kP_{k|k-1}C_k^T)^{-1}$$

3. Update the estimated states:

$$\hat{x}_{k|k} = \hat{x}_{k|k-1} + L_k(y_k - \hat{y}_{k|k-1})$$

4. Update the error covariance matrix:

$$P_{k|k} = (I_n - L_kC_k)P_{k|k-1}$$

4 The Ensemble Kalman Filter

The ensemble Kalman filter is a sequential data assimilation method where the error statistics are predicted by solving the Fokker-Planck equation (35), which describes the time evolution of a probability density function of a model state, using a Monte Carlo or ensemble integration. The method was originally proposed by [3]. By integrating an ensemble of model states forward in time it is possible to calculate statistical moments like mean and error covariances whenever such information is required. Thus, all the statistical information about the predicted model state that is required at analysis times is contained in the ensemble.

The method is presented in three stages:

- Representation of error statistics
- Prediction of error statistics
- The estimation problem

4.1 Representation of Error Statistics

The error covariance matrices for the prior and the current estimate, $P_{k|k-1}$ and $P_{k|k}$, are in the Kalman filter defined in terms of the true state as

$$P_{k|k-1} = E\big[(x_k - \hat{x}_{k|k-1})(x_k - \hat{x}_{k|k-1})^{\mathrm{T}}\big] \tag{23}$$

$$P_{k|k} = E\big[(x_k - \hat{x}_{k|k})(x_k - \hat{x}_{k|k})^{\mathrm{T}}\big] \tag{24}$$

where $E[\cdot]$ denotes an expectation value. Now, for the EnKF assume that we have an ensemble of forecasted model states that randomly sample the model errors at time k. Let's denote this ensemble as $\boldsymbol{X}_{k|k-1}$ and is defined by

$$\boldsymbol{X}_{k|k-1} \stackrel{\triangle}{=} (\hat{x}^1_{k|k-1}, \ldots, \hat{x}^N_{k|k-1}), \tag{25}$$

where the superscript denotes the ensemble member. Then, the ensemble mean $\bar{\hat{x}}_{k|k-1}$ is defined by

$$\bar{\hat{x}}_{k|k-1} \stackrel{\triangle}{=} \frac{1}{N}\sum_{i=1}^{N} \hat{x}^j_{k|k-1}. \tag{26}$$

Since the true state x_k is not known, and in order to write (23) and (24) in terms of (25), we therefore define the ensemble covariance matrices around the ensemble mean as follows; define the ensemble of prior estimation errors by

$$\boldsymbol{E}_{k|k-1} \stackrel{\triangle}{=} (\hat{x}^1_{k|k-1} - \bar{\hat{x}}_{k|k-1}, \ldots, \hat{x}^N_{k|k-1} - \bar{\hat{x}}_{k|k-1}), \tag{27}$$

and the ensemble of estimation errors by

$$\boldsymbol{E}_{k|k} \stackrel{\triangle}{=} (\hat{x}^1_{k|k} - \bar{\hat{x}}_{k|k}, \ldots, \hat{x}^N_{k|k} - \bar{\hat{x}}_{k|k}). \tag{28}$$

Hence,

$$P_{k|k-1} \approx \hat{P}_{k|k-1} \stackrel{\triangle}{=} \frac{1}{N-1} E\big[\boldsymbol{E}_{k|k-1}\boldsymbol{E}^{\mathrm{T}}_{k|k-1}\big], \tag{29}$$

$$P_{k|k} \approx \hat{P}_{k|k} \stackrel{\triangle}{=} \frac{1}{N-1} E\big[\boldsymbol{E}_{k|k}\boldsymbol{E}^{\mathrm{T}}_{k|k}\big], \tag{30}$$

which are averages over the ensembles. Thus, we can use an interpretation where the ensemble mean is the best estimate and the spreading of the ensemble around the mean is a natural definition of the error in the ensemble mean. Since the error covariances defined in (29) and (30) are defined as ensemble averages, there will clearly exist infinitively many ensembles with an error covariance equal to $\hat{P}_{k|k-1}$ and $\hat{P}_{k|k}$. Thus, instead of storing a full covariance matrix, we can represent the same error statistics using an appropriate ensemble of model states. Given an error covariance matrix, an ensemble of finite size will always provide an approximation to the error covariance matrix. However, when the size of the ensemble N increases the errors in the Monte Carlo sampling will decrease proportional to $1/\sqrt{N}$.

Suppose now that we have N model states in the ensemble, each of dimension n. Each of these model states can be represented as a single point in an N-dimensional state space. All the ensemble members together will constitute a cloud of points in the state space. Such a cloud of points in the state space can, in the limit when N goes to infinity, be described using a probability density function

$$\phi(x) = \frac{dN}{N}, \tag{31}$$

where dN is the number of points in a small unit volume and N is the total number of points. With knowledge about either or the ensemble representing we can calculate whichever statistical moments (such as mean, covariances etc.) we want whenever they are needed.

The conclusion so far is that the information contained by a full probability density function can be exactly represented by an infinite ensemble of model states.

4.2 Prediction of Error Statistics

The EnKF was designed to resolve two major problems related to the use of the extended Kalman filter (EKF) with nonlinear dynamics in large state spaces. The first problem relates to the use of an approximate closure scheme in the EKF, and the other to the huge computational requirements associated with the storage and forward integration of the error covariance matrix. The EKF applies a closure scheme where third- and higher order moments in the error covariance equation are discarded. This linearization has been shown to be invalid in a number of applications. In fact, the equation is no longer the

fundamental equation for the error evolution when the dynamical model is nonlinear. For a nonlinear model where we appreciate that the model is not perfect and contains model errors, we can write it as a discrete-time stochastic differential equation as

$$x_{k+1} = \mathcal{A}(x_k) + \eta_k \tag{32}$$

with η_k the model error at time k defined by

$$\eta_k \triangleq \boldsymbol{G}_k(x_k)\delta_k, \tag{33}$$

with $\boldsymbol{G}_k(x_k) \in \mathbb{R}^{n\times l}$ is a state-dependent matrix, where the covariance matrix $Q_k \in \mathbb{R}^{n\times n}$ is defined as

$$Q_k \triangleq E[\boldsymbol{G}_k(x_k)\boldsymbol{G}_k(x_k)^{\mathrm{T}}], \tag{34}$$

and $\delta_k \in \mathbb{R}^l$ is a process we want to approximate as white noise. Equation (32) implies that even if the initial state is known precisely, future model sates cannot since unknown random model errors are continually added.

Conceptually, the evolution of (31) can be modelled with the Fokker-Planck equation

$$\frac{\partial\phi(x_k)}{\partial t} = -\nabla\cdot\big[\mathcal{A}(x_k)\phi(x_k)\big] + \sum_{i,j}\frac{\partial^2}{\partial x_{k(i)}\partial x_{k(j)}}\big(\frac{Q_k}{2}\big)_{ij}\phi(x_k) \tag{35}$$

This equation does not apply any important approximations and can be considered as the fundamental equation for the time evolution of error statistics. A detailed derivation is given in [5]. The equation describes the change of the probability density in a local volume which is dependent on the divergence term describing a probability flux into the local volume (impact of the dynamical equation) and the diffusion term which tends to flatten the probability density due to the effect of stochastic model errors. If (35) could be solved for the probability density function, it would be possible to calculate statistical moments like the mean state and the error covariance for the model forecast to be used in the analysis scheme. The EnKF applies a so called Markov Chain Monte Carlo (MCMC) method to solve (35). The probability density can be represented using a large ensemble of model states. By integrating these model states forward in time according to the model dynamics described by (32), this ensemble prediction is equivalent to solving the Fokker-Planck equation using a MCMC method. This procedure forms the backbone for the EnKF.

4.3 The Estimation Problem

In the standard KF estimation problem the definition of $P_{k|k-1}$ and $P_{k|k}$ are used. It is now given a derivation of the estimation problem for the EnKF using (29) and (30).

The EnKF performs an ensemble of parallel data assimilation cycles, using (11) as follows,

for $i = 1, \ldots, N$

$$\hat{x}^i_{k|k} = \hat{x}^i_{k|k-1} + L_{e_k}\big(y^i_k - \mathcal{C}(\hat{x}^i_{k|k-1})\big), \tag{36}$$

where $\mathcal{C}$ is the observation operator, which is permitted to be a nonlinear operator, and the observations $y^i_k = y_k + \epsilon^i$ are perturbed observations defined such that $\epsilon^i \sim \mathcal{N}(0, R_e)$. In the limit of an infinite ensemble the matrix R_e will converge toward the prescribed error covariance matrix R used in the standard KF.

Similar to the standard KF, In (36) $L_{e_k}$is defined as

$$L_{e_k} = \hat{P}_{k|k-1}\mathcal{C}^{\mathrm{T}}(\mathcal{C}\hat{P}_{k|k-1}\mathcal{C}^{\mathrm{T}} + R_e)^{-1}, \tag{37}$$

with the difference that $\mathcal{C}$ can be nonlinear which is a powerful advantage compare to other non-linear KF that are based on linearized models like EKF. Envision a situation where errors grow rapidly but saturate at low amplitude; the linear assumption of error growth in the EKF will result in an overestimate of the prior error variance, but the differences among ensemble members will not grow without bound and thus should provide a more accurate model of the actual prior error statistics.

On the other hand, for a complex model with a high-dimensional state vector, explicitly forming $\hat{P}_{k|k-1}$ as in (29) would be computationally prohibitive. However, in the EnKF, L_{e_k} can be formed without ever explicitly computing the full $\hat{P}_{k|k-1}$. Instead, the components of $\hat{P}_{k|k-1}\mathcal{C}^{\mathrm{T}}$ and $\mathcal{C}\hat{P}_{k|k-1}\mathcal{C}^{\mathrm{T}}$ of L_{e_k} are computed separately. Define

$$\overline{\mathcal{C}(\hat{x}_{k|k-1})} \triangleq \frac{1}{N}\sum_{i=1}^{N}\mathcal{C}(\hat{x}^i_{k|k-1}), \tag{38}$$

which represents the mean of the estimate of the observation interpolated from the background forecasts. Then

$$\hat{P}_{k|k-1}\mathcal{C}^{\mathrm{T}} \triangleq \frac{1}{N-1}\sum_{i=1}^{N}\big(\hat{x}^i_{k|k-1} - \bar{\hat{x}}_{k|k-1}\big)\big(\mathcal{C}(\hat{x}^i_{k|k-1}) - \overline{\mathcal{C}(\hat{x}_{k|k-1})}\big)^{\mathrm{T}}, \tag{39}$$

and

$$\mathcal{C}\hat{P}_{k|k-1}\mathcal{C}^{\mathrm{T}} \triangleq \frac{1}{N-1}\sum_{i=1}^{N}\big(\mathcal{C}(\hat{x}^i_{k|k-1}) - \overline{\mathcal{C}(\hat{x}_{k|k-1})}\big)\big(\mathcal{C}(\hat{x}^i_{k|k-1}) - \overline{\mathcal{C}(\hat{x}_{k|k-1})}\big)^{\mathrm{T}}, \tag{40}$$

After the estimation is done, a short-range forecast is computed by running the physics first principle based model (32) until new measurements are taken, then the data assimilation is repeat it.

5 Numerical Results

In order to investigate how the EnKF operates in MHD systems, we took the ideal MHD system equations (1)-(6) with (8), setting the boundary conditions of the right-hand side such that it simulates the magnetosphere around the earth. This system was simulated with the VAC code with the following parameters:

- Grid size: 34×54
- Initial conditions of the state space variables:
  - Mass density, $\rho = 1.0Kg/m^3$
  - Velocity in x- and y-directions, $V_x = 20m/s$, $V_y = 0m/s$
  - Pressure, $p = 1.0Kg/ms^2$
  - Magnetic field in x- and y-directions, $B_x = 0mT$, $B_y = 1.0mT$
- ratio of specific heats, $\gamma = 5/3$
- Simulation sample time, 1×10^{-4} seconds
- Data assimilation sample time, 4×10^{-4} seconds
- Spatial discretization method, Total Variation Diminishing Lax-Friedrich, TVDLF.

As a result the order of the system is 11016, 6 state space variables and 34×54 gridpoints. To excite the system, a square sinusoidal wave for B_y and V_x was generated at the left-hand boundary, simulating a magnetic storm. The variation of B_y were from 1 to 1.5 mT while for V_x from 20 to 30 m/s.

Figure 1 depicts a general scheme of the EnKF implementation by running Matlab and the VAC code simultaneously. Since we can see in the scheme we did not need any extra code for the model, anyhow we had to write the code of the EnKF in Matlab, and some code to read and write the VAC's files where the initial and final conditions in each data-assimilation time-step are saved. As a result, we have got an modular data-assimilation system where the nonlinear model integration module is executed by the VAC code, while the data assimilation module for Matlab. This is one of the motivation for using the EnKF, because it is quite straightforward to implement, and the results are very confident.

To investigate the performance of the EnKF in MHD systems a magnetic storm around the earth was simulated by changing the boundary conditions as mentioned above. We study three cases, for 10, 100, and 200 measurement points, and for each case we use 50, 150, and 300 ensemble members, respectively.

Figure 2 shows the root mean square error (RMSE) of the state space estimation for the whole scenarios. On the first column, when 50 ensemble members are used, can be seen that the data assimilation process always crashes independent of the number of measurement points, this is due to the fact that the number of ensemble members is small compare to the order or the system, hence, it is difficult for the EnKF to describe very

well the statistics of system, taking the system to regions where the model integration becomes unfeasible.

In the other cases, 150 and 300 members, the data assimilation process works more reliable, even for the cases with 10 measurement points. Although the worst performance is for the case of 10 measurement points with 150 and 300 ensemble members, the results are closed to the other cases indicating that the number of ensemble members is more important than the number of measurement points; however the number and the location of the measurement points is important as well. In the experiments the location of the measurement point are chosen such that at least half of the points were located in the right-half plane around the bowshock where the more drastic changes occurs, this guarantees that the data assimilation process will track the big changes in the system, otherwise the estimation would be very poor.

Figures 3-5, and 6-8 depict how the magnetic field and the plasma velocity around the earth are estimated respectively for the different cases. It can be seen clearer that the more ensemble members and measurement points are taken, the better the estimation is, as expected.

6 Conclusions

In this paper we introduced a new area of application for the EnKF, *space weather forecast*. The EnKF is an extension of the Kalman filter to the nonlinear case, where based on a Monte Carlo simulation approach the measurement and process noise errors are propagated. One of the advantages of the EnKF is its facility to be implemented as a modular system, with mainly two modules, namely, the model simulator and the data assimilation module. This scheme permits the use of specialized codes for each task, making the EnKF more robust and reliable.

The EnKF performed very well in the experiment shown. The results are very promising in the sense that with few measurement points located strategically, we can obtain a good estimation of the dynamics of the system. We mention this, because in the real case there are very few satellites out there in the space which can be used as measurement points.

One of the drawbacks of the EnKF is that it is very demanding computationally, despite the fact that one can represent the statistics with a few number of ensemble members compared to the size of the system. Also the knowledge of the process and measurement noise are needed in order to have more accurate results.

7 Acknowledgment

Dr. Bart De Moor is a full professor at the Katholieke Universiteit Leuven, Belgium. Research supported by Research Council KUL: GOA-Mefisto 666, GOA-Ambiorics, several PhD/postdoc & fellow grants; Flemish Government: - FWO: PhD/postdoc grants, projects, G.0240.99 (multilinear algebra), G.0407.02 (support vector machines), G.0197.02

(power islands), G.0141.03 (Identification and cryptography), G.0491.03 (control for intensive care glycemia), G.0120.03 (QIT), G.0452.04 (QC), G.0499.04 (robust SVM), research communities (ICCoS, ANMMM, MLDM); - AWI: Bil. Int. Collaboration Hungary/ Poland; - IWT: PhD Grants, GBOU (McKnow) Belgian Federal Government: Belgian Federal Science Policy Office: IUAP V-22 (Dynamical Systems and Control: Computation, Identification and Modelling, 2002-2006), PODO-II (CP/01/40: TMS and Sustainibility); EU: FP5-Quprodis; ERNSI; Eureka 2063-IMPACT; Eureka 2419-FliTE; Contract Research/agreements: ISMC/IPCOS, Data4s, TML, Elia, LMS, IPCOS, Mastercard.

References

[1] G.P. Burgers, P.J Van Leeuwen and G. Evensen, Analysis scheme in the ensemble Kalman filter, Monthly Weather Review, 1998, vol. 126, pp. 1719-1724.

[2] R. Dendy, Plasma Physics: an Introductory Course, 1st edition, Cambridge University Press, 1996.

[3] G. Evensen, Sequential data assimilaion with a nonlinear quasigeostrophic model using Monte Carlo methods to forecast error statistics, Geophys. Res., 1994, vol. 99-C5, pp. 10143-10162.

[4] G. Evensen, The ensemble Kalman filter: theroretical formulation and practical implementation, Ocean Dynamics, 2003, vol. 53, pp. 343-367.

[5] A.H. Jazwinski, Stochastic processes and filtering theory, Academic Press, 1970.

[6] R.E. Kalman, A new approach to linear filtering and prediction problems, Transactions of hte AMSE-Journal of Basic Engineering, 1960, vol. 83D, pp. 35-45.

[7] R.E. Kalman and R.S. Bucy, New results in linear filtering and prediction theory, Transactions of hte AMSE-Journal of Basic Engineering, 1961, vol. 83D, pp. 95-108.

[8] G. Tóth and R. Keppens, Versatile Advection Code, Universiteit Utrecht, The Netherlands, 2003.

[9] A.C. Lorenc, Analysis methods for numerical weather prediction, Quart. J. Roy. Meteor. Soc., 1986, vol. 112, pp. 1177-1194.

[10] D.F. Parrish and J.C. Derber, The National Meteorological Center's Spectral Statistical Interpolation Analysis System, Monthly Weather Review, 1992, vol. 120, pp. 1747-1763.

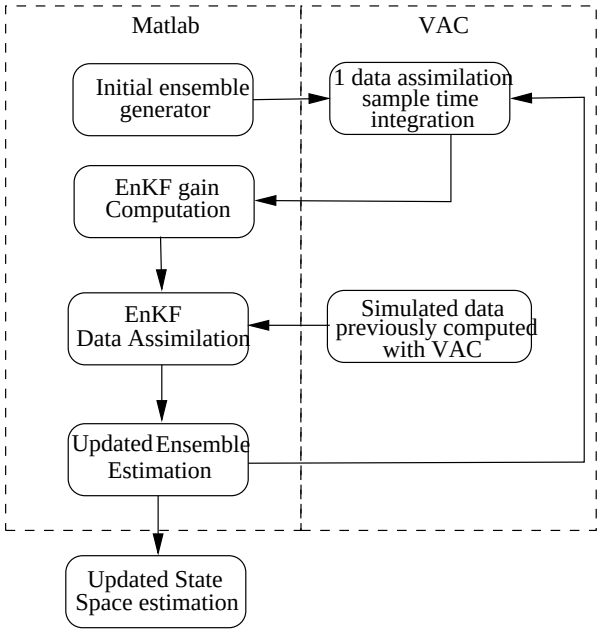

Figure 1: Block diagram scheme of the EnKF implementation using VAC and Matlab.

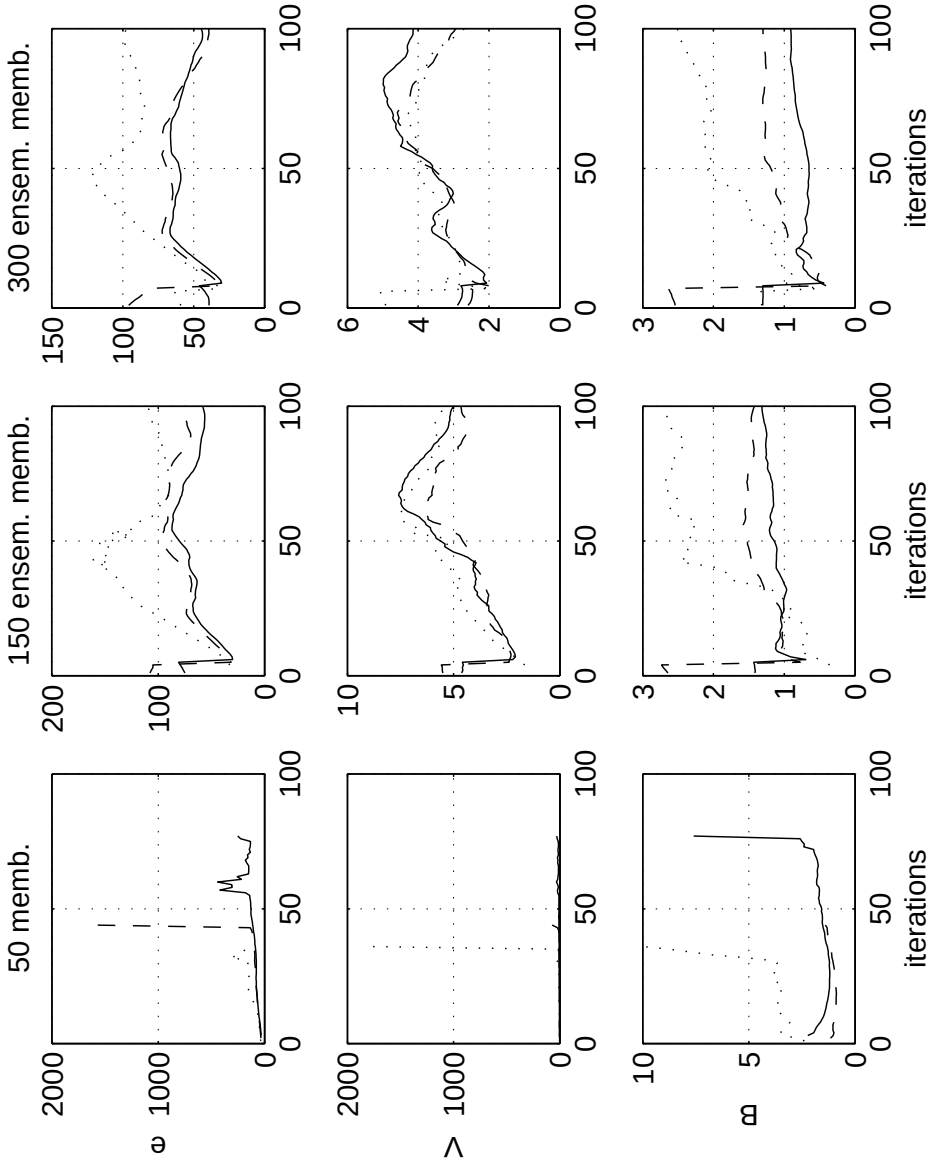

Figure 2: Comparison of the performance of the EnKF for different number of measurement points as well as ensemble members, where e-energy density, V-velocity, and B-Magnetic field. Dotted line; RMSE for 10 measurement points, dashed line; RMSE for 100 measurement points, and solid line; RMSE for 200 measurement points.

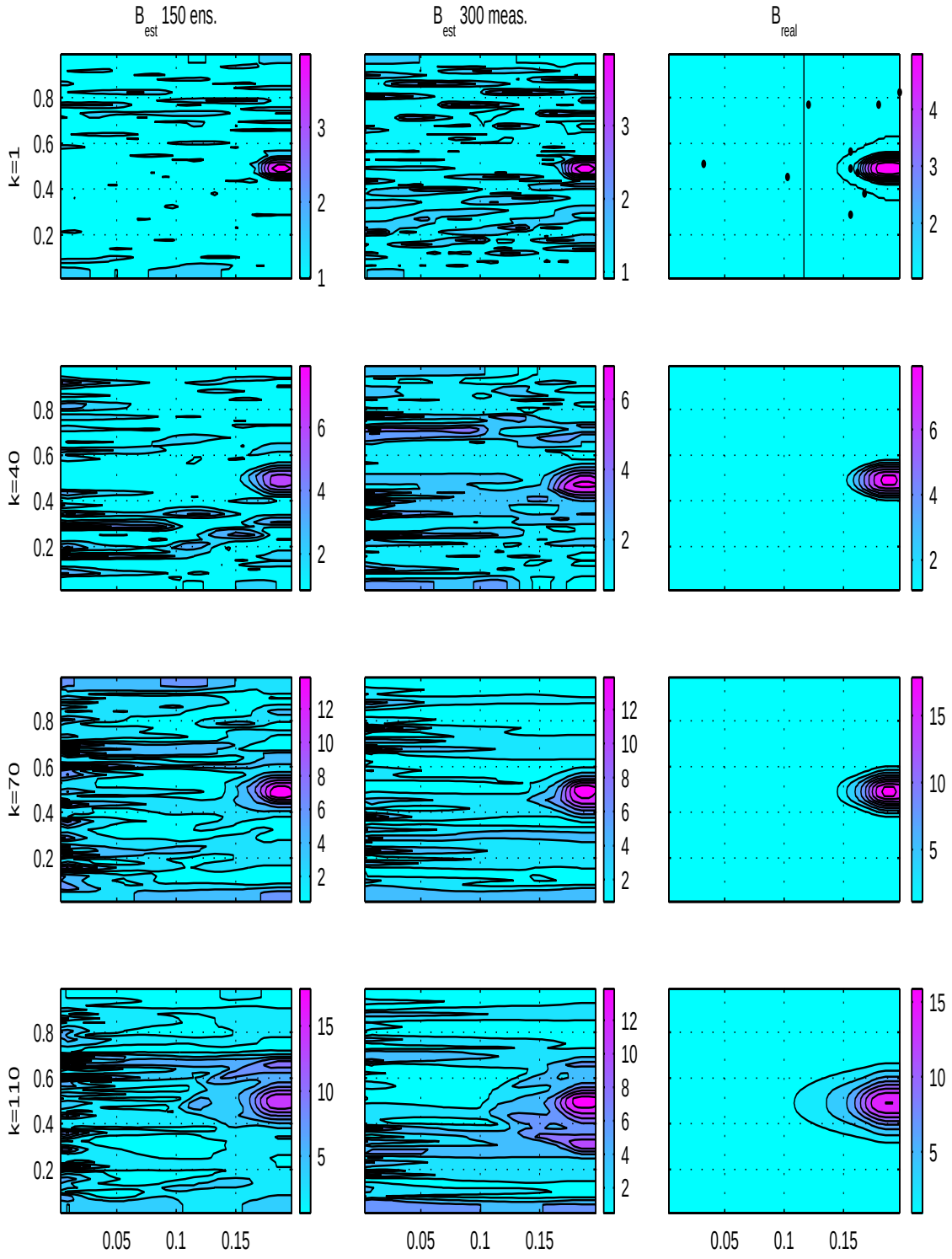

Figure 3: Comparison of performance for the case of 10 measurement points. At the top-right, the big dots are the location of the measurement points on the grid.

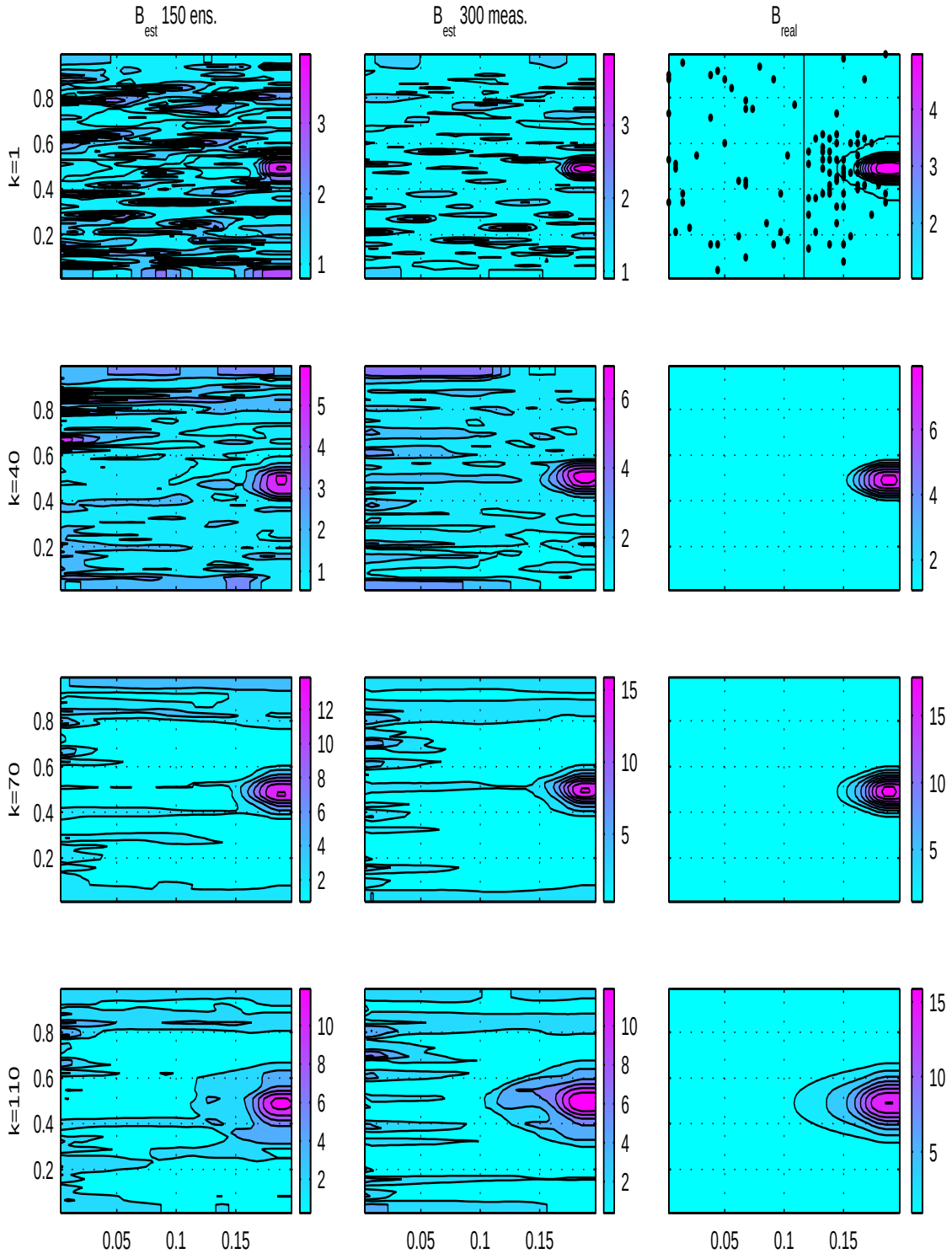

Figure 4: Comparison of performance for the case of 100 measurement points. At the top-right, the big dots are the location of the measurement points on the grid.

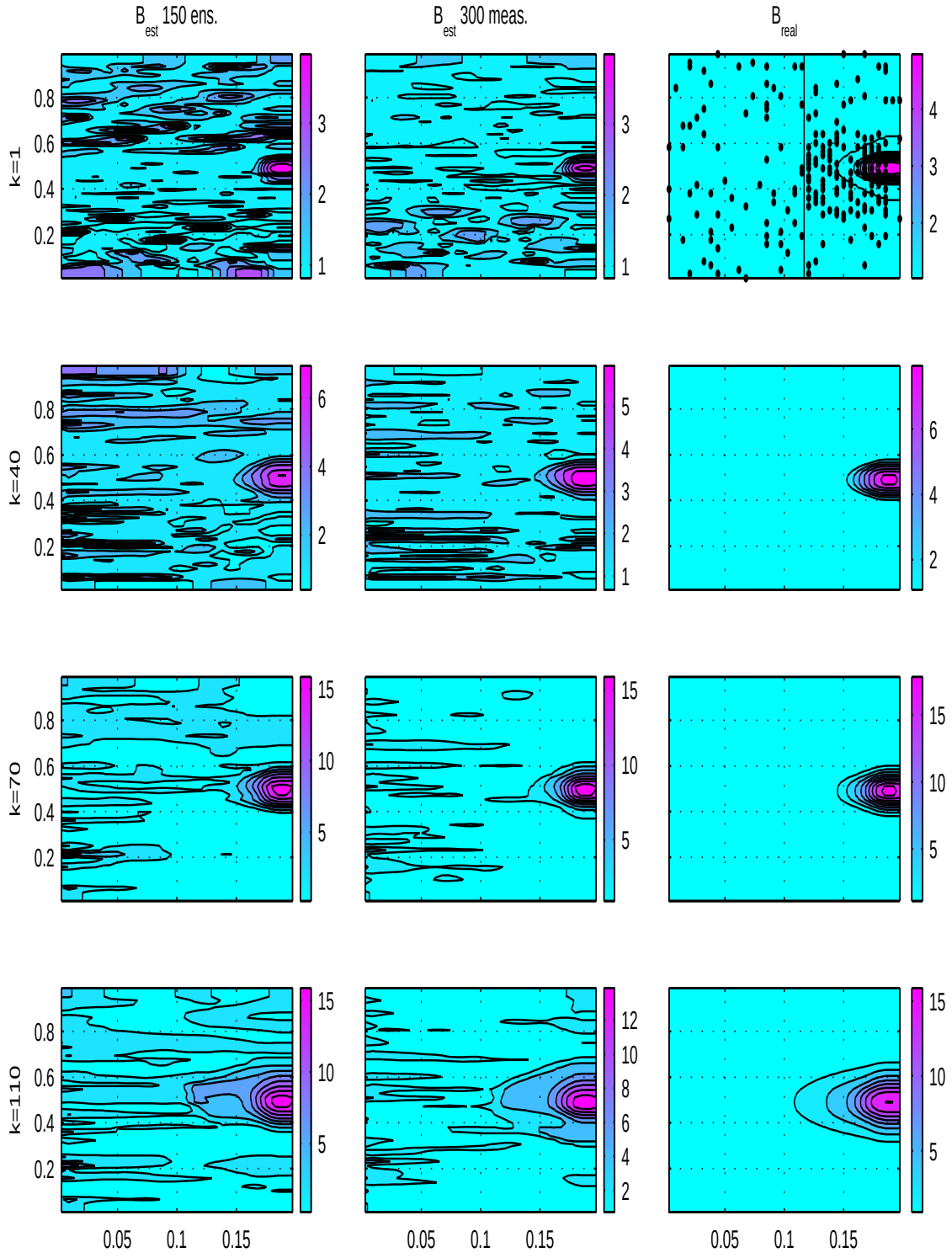

Figure 5: Comparison of performance for the case of 200 measurement points. At the top-right, the big dots are the location of the measurement points on the grid.

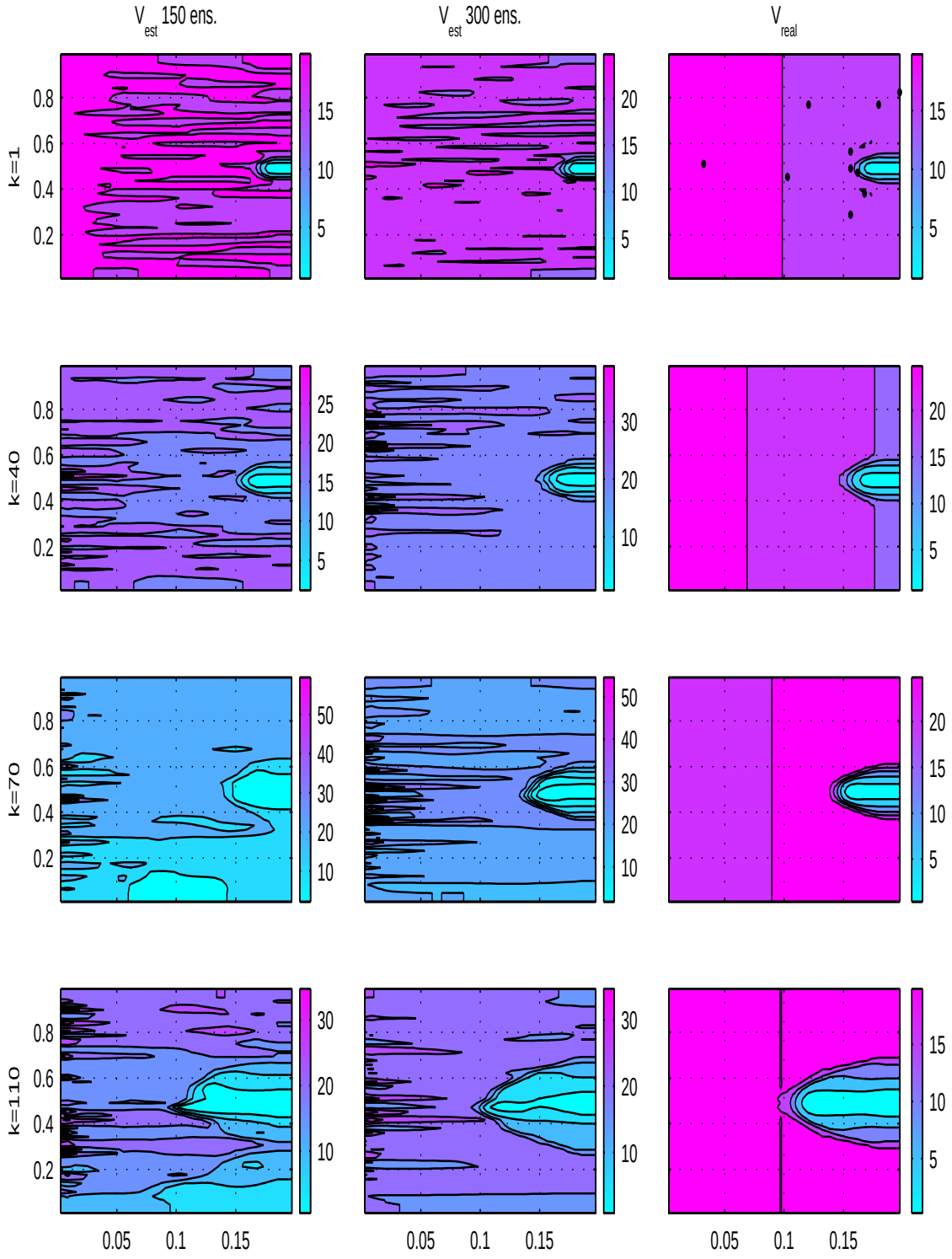

Figure 6: Comparison of performance for the case of 10 measurement points. At the top-right, the big dots are the location of the measurement points on the grid.

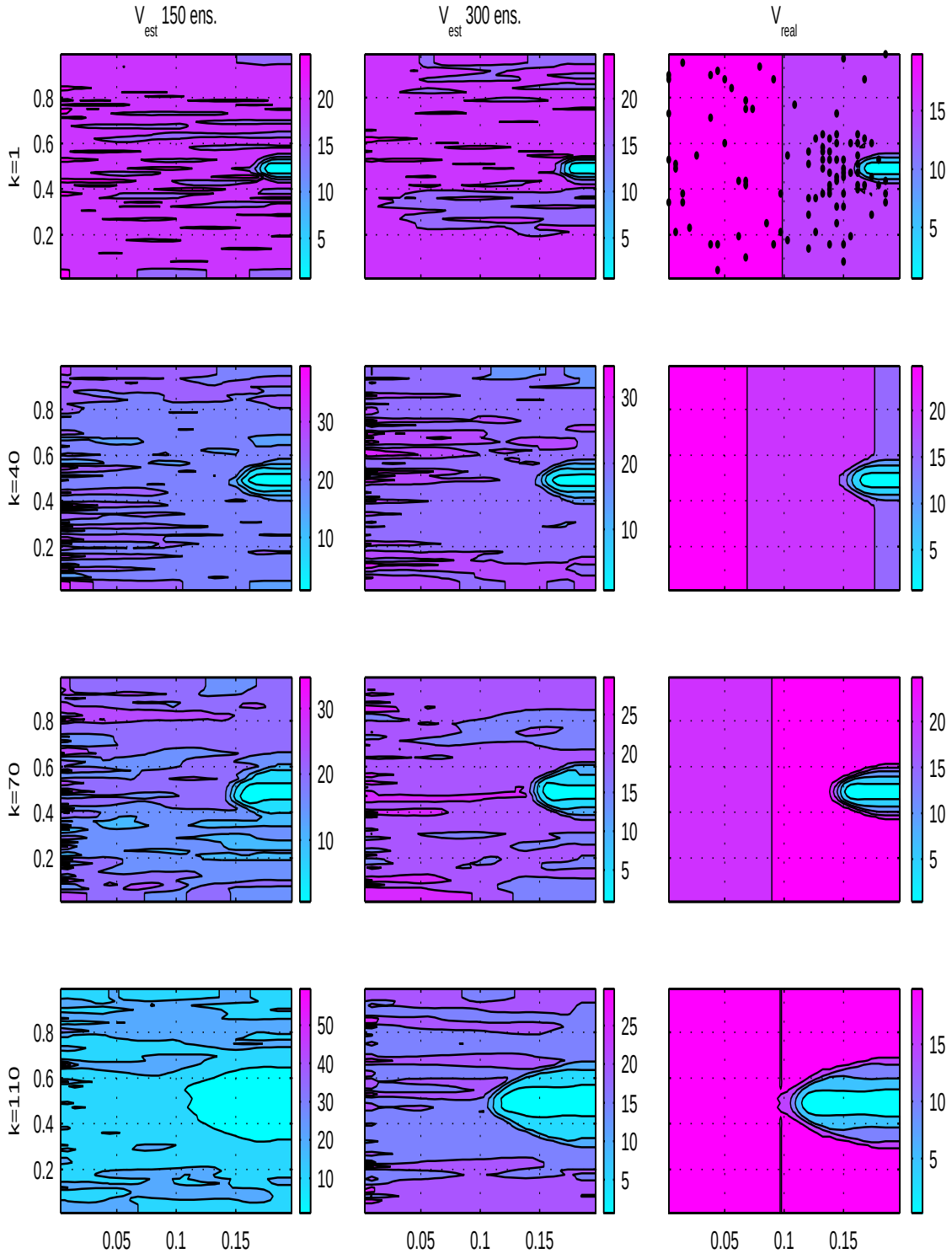

Figure 7: Comparison of performance for the case of 100 measurement points. At the top-right, the big dots are the location of the measurement points on the grid.

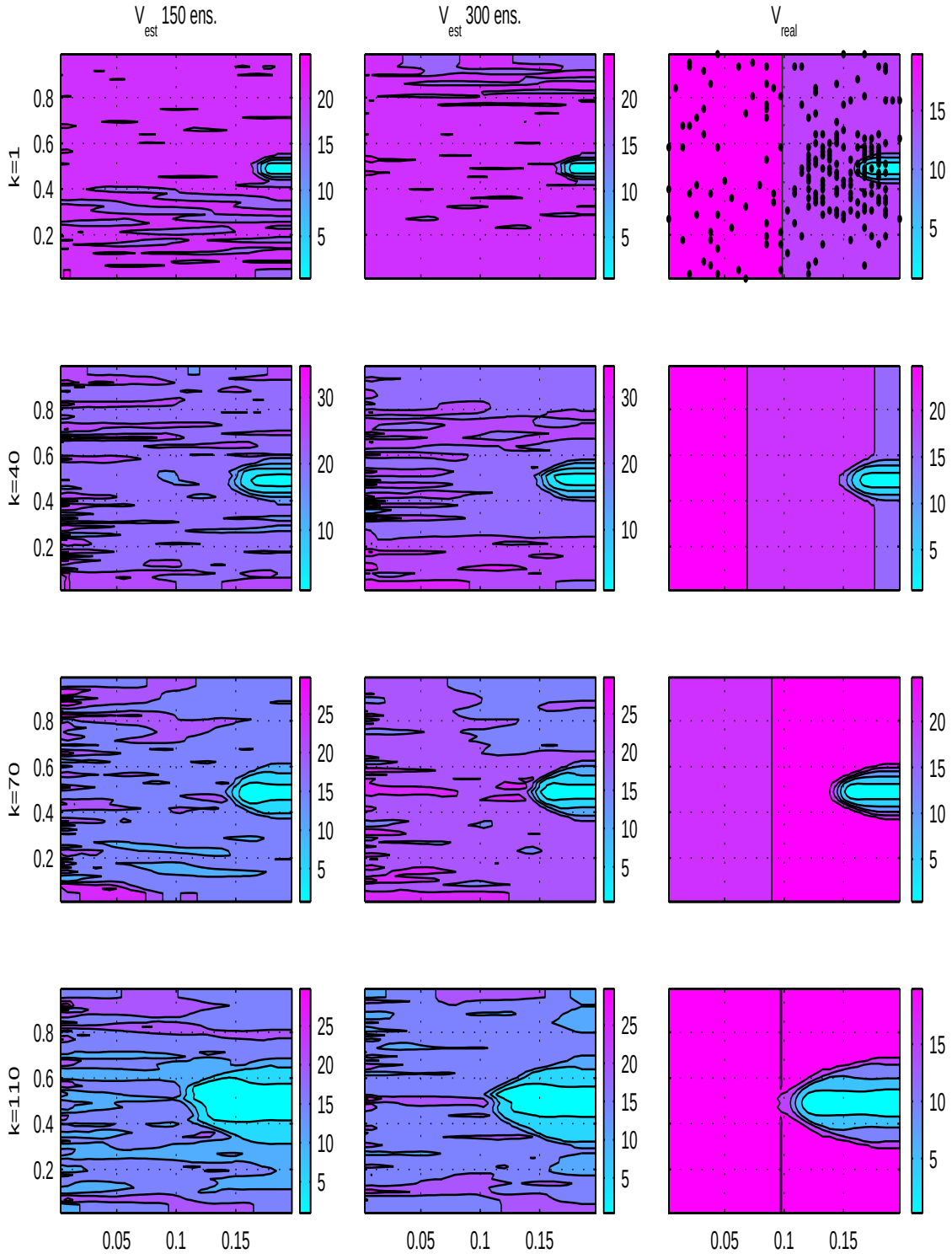

Figure 8: Comparison of performance for the case of 200 measurement points. At the top-right, the big dots are the location of the measurement points on the grid.